

Blossom Morphology and Correlative Performance Improvement of Recycled Polyethylene/Wood Flour Composites with Steam-Activated Interfaces

Haoqun Hong,^{a,b} Hao Liu,^a Haiyan Zhang,^{a,b,*} Hui He,^c Tao Liu,^d and Demin Jia^c

Interfacial compatibility plays a key role in the performances of natural fiber-reinforced composites. The measures commonly used to improve the interfacial compatibility focus more on the addition of various compatibilizers than on the structural modification of the natural fiber. In this paper, an attempt was made to enlarge the interfacial interaction areas of the recycled polyethylene (rPE)/wood flour (WF) composites by steaming the WF. Multi-monomer graft copolymers of polyethylene (GPE) were used as compatibilizers for the composites. How the enlarged interfaces affected the morphology, mechanical properties, water resistance, thermal stability, and dynamic rheological properties of the rPE/WF composites was investigated. The steaming process was able to enlarge the voids of the WF and therefore activate more interfaces for interactions. It was found that the interfacial morphology of the composites was affected by the degree of interfacial compatibility of the composites and so was characterized by various distinctive blossom shapes having a variation of compositions. With the help of GPE, the steaming process was able to significantly improve the interfacial compatibility of the composites and therefore improve the mechanical properties, water resistance, thermal stability, and dynamic rheological properties of the composites.

Keywords: Polymer-matrix composites; Recycling; Polymers; Wood; Interface; Graft copolymers

Contact information: a: School of Materials and Energy, Guangdong University of Technology, Guangzhou 510006, China; b: Guangdong Provincial Key Laboratory of Functional Soft Condensed Matter, Guangdong University of Technology, Guangzhou 510006, China; c: College of Materials Science and Engineering, South China University of Technology, Guangzhou 510640, China; d: Product Research & Development Center, Guangzhou LESCO-KINGFA WPC Technology Co., Ltd, Guangzhou 510520, China; *Corresponding author: hyzhang@gdut.edu.cn

INTRODUCTION

With the ongoing energy crisis and environmental deterioration, the recycling and reuse of wastes and by-products have become important measures for conserving resources and protecting the environment (Thompson *et al.* 2009; Najafi 2013). Preparing specific, useful products is one of the most effective means of recycling and reusing these wastes and by-products. Among these useful products, wood-plastic composites (WPC) are one of the most attractive because they provide a promising use for both recycled plastics and forestry and agricultural by-products in the preparation of valuable composites by means of conventional polymer processing and fabricating machines such as the extruder (Guo and Wang 2008; Wu *et al.* 2014) and intensive mixer (Fang *et al.* 2013). The polymers most frequently used to prepare WPC are thermoplastics such as polypropylene (PP) (Gao and Wang 2008), polyethylene (PE) (Ou *et al.* 2010; Xu *et al.* 2010; Gao *et al.* 2012; Wu *et al.* 2014; Zhou *et al.* 2014), polyvinyl chloride (PVC) (Xu *et al.* 2010; Fang *et al.* 2013),

and polystyrene (PS) (Nair and Thomas 2003; Mansour *et al.* 2006). The by-products of preparing WPC are natural cellulosic fillers such as wood flour (WF), bamboo flour, oil palm fiber, sisal fiber, rice chaff, and bagasse (Ashori 2008). Thus, WPC has the advantages of ease of manufacture, environmental safety, biodegradability, low cost, and high strength. It has been widely applied in the construction, automotive, packaging, and other industries (Ashori 2008; Thompson *et al.* 2009; Najafi 2013).

However, most polymers used for WPC are hydrophobic, and natural fillers are hydrophilic. The hydrophobic polymers are weakly compatible with the hydrophilic natural fillers at their interfaces (Bledzki and Gassan 1999; Guo *et al.* 2013). These weakly compatible interfaces result in the low performance of WPC. To successfully prepare a high-performance WPC, the interfacial compatibility between the polymers and natural fillers has to be addressed. The interfacial compatibility of WPC has been improved by modifying natural fillers with acetylation (Zafeiropoulos *et al.* 2002; Mbarek *et al.* 2013), alkali (Aziz and Ansell 2004), organosilane (Demir *et al.* 2006), or using compatibilizers (Kazayawoko *et al.* 1999; Artzi *et al.* 2003; Manchado *et al.* 2003; Bengtsson *et al.* 2007; Danyadi *et al.* 2007; Guo and Wang 2008; Ashori and Nourbakhsh 2009; Lashgari *et al.* 2011; Gao *et al.* 2012; Hoang *et al.* 2013; Zhou *et al.* 2014).

Of those methods, using compatibilizers such as graft copolymers, which chemically and physically enhance the interfacial interactions between the polymers and natural fibers, has been shown to be an effective method for improving the interfacial compatibility (Bledzki and Gassan 1999; Li *et al.* 2007; Guo and Wang 2008; Lashgari *et al.* 2011; Gao *et al.* 2012). Moreover, using graft copolymers such as the compatibilizers is a convenient and attractive method of preparing WPC in that it can facilitate the WPC preparation procedure by directly blending the natural fibers with the polymer matrix and compatibilizers. The most popular graft copolymers for use with WPC are those such as maleated polyolefins (Kazayawoko *et al.* 1999; Manchado *et al.* 2003; Demir *et al.* 2006; Gao *et al.* 2012; Zhou *et al.* 2014), because these graft copolymers can facilitate strong interfacial interactions between the polymers and natural fibers by means of the esterification reaction between maleic anhydride (MAH) and the hydroxyl groups of natural fibers (Guo *et al.* 2013). However, most WPC is filled with more than 50 wt.% natural fibers in order to reduce the cost of WPC. Higher filler contents tend to worsen the performance of WPC and challenge the compatibilizing capability of compatibilizers. The graft degrees of maleated polyolefins are not high enough to confer efficient interfacial interactions to a highly filled composite because MAH is difficult to homo-polymerize at higher temperature (Li *et al.* 2001). To maintain acceptable performance levels for WPC, attempts have been made to improve the compatibilizing capability of compatibilizers, by such methods as the *in situ* reactive compatibilization (Li *et al.* 2012), synergistic compatibilization (Gao *et al.* 2012; Yeh *et al.* 2013), and use of a multi-monomer graft copolymer (Jia *et al.* 2000; Ding *et al.* 2005; Hong *et al.* 2009; Hong *et al.* 2011). The multi-monomer graft copolymer is one of the most efficient compatibilizers, and is prepared by grafting MAH with one or two co-monomers onto the melting or solid state polyolefin so as to increase the graft degree of MAH and thereby improve the compatibilizing capability of the graft copolymer (Ding *et al.* 2005; Hong *et al.* 2009; Hong *et al.* 2011) through chemical or physical interaction at the interfaces (Bledzki and Gassan 1999).

However, the interfacial compatibility and performance of WPC are associated not only with the use of compatibilizers but also with the structure of the natural fibers (Liu *et al.* 2014; Ou *et al.* 2014a,b). Ou *et al.* (2014b) studied the influence of the removal of

hemicelluloses and lignin (together or respectively) from wood flours on the mechanical properties, dimensional stability, and rheological properties of wood particle/high density polyethylene composites. They found that these performances were influenced by the cell wall composition of the wood particles (Ou *et al.* 2014a,b). Moreover, it was found that high filler content usually causes the aggregation of natural fibers, such as wood particles, in the WPC (Danyadi *et al.* 2007). The aggregated natural fillers usually have gaps among them, in addition to the cavities and capillaries on their coarse surfaces, which originate from their grinded cellular structure. These voids cannot be easily accessed by the polymer chains without any modification to the natural fibers (Ou *et al.* 2014b). WPC can be improved not only by improvements in the interfacial interactions at the coarse surfaces of the natural fillers, but also by improvements in the interfacial interactions at these voids. This means that the interfacial interactions of WPC could either be enhanced by improving the infiltration of compatibilizers into these voids or by enlarging the voids for the fillers. In order to enhance the interfacial interactions at these minimally accessible locations, alkali and glycerin solutions have been used to pre-treat and modify natural fibers. This pre-treatment method has improved the interfacial compatibility of WPC (Aziz and Ansell 2004; Luo *et al.* 2014). Recently, the compounds of two complementary multi-monomer graft copolymers with improved infiltrating capability were used to compatibilize the recycled polyethylene (rPE)/WF composites and achieve satisfactory improvements in performance (Hong *et al.* 2014). However, whether it is possible to enhance the interfacial interactions by manipulating the interfacial interaction areas of the natural fibers without changing the infiltrating capability of the compatibilizers, such that the compatibilizers can easily infiltrate into the voids of natural fibers, remains unchallenged in the literature.

In this paper, an attempt was made to enlarge the interfacial interaction areas of WPC by steaming the wood flours. This enlarged the voids of the steamed wood flours (SWF), into which the compatibilizer could easily infiltrate. The infiltrated voids significantly enhanced the interfacial interactions. How the enhanced interfacial interactions affected the morphology, mechanical properties, water resistance, thermal stability, and rheological properties of rPE/WF composites was investigated.

EXPERIMENTAL

Materials

Recycled polyethylene (rPE), with a melting flow rate (MFR) of 2.12 g/min, was supplied by Dongguan Dada Co., Ltd and used as received. The WF was obtained from the aspen (*Populus tremuloides*) wood that was provided by Jiangmen Weihua Co., Ltd. The steamed wood flour (SWF) was prepared by steaming WF in a boiling pot for 1 h. The ternary graft copolymers of polyethylene (GPE) were used as the compatibilizers for rPE/WF composites. GPE with a 10.5% graft degree was synthesized *via* solid phase grafting of MAH, MMA, and BA (the mass ratio of the MAH/MMA/BA was 6/4/2) onto powdered PE initiated by benzoyl peroxide (BPO) at 120 °C (Jia *et al.* 2000).

Methods

Preparation of rPE/WF composites

The WF-filled rPE composites were prepared on a two-roll mill whose roll diameter was 16 cm. While the rolls were being heated, rPE was first added onto the running rolls and plasticized for 3 min. GPE and WF were then added successively onto the melted rPE

and mixed for 5 min. The loadings of GPE and the fillers were 7 phr (parts per hundred rPE in weight) and 50 wt.%, respectively. The melted composites were compressed into $250 \times 250 \times 4$ mm plates on a 25-ton flat vulcanizer. The plates were cooled at room temperature for 24 h before tailoring and testing.

Measurements

The tensile and flexural tests were carried out on a universal testing machine (DCS-5000, Shimadzu, Japan) at room temperature according to ISO527-2: 1993 (with dumbbell sample dimensions of $170 \times 10 \times 4$ mm) and ISO178: 2001 (with sample dimensions of $80 \times 10 \times 4$ mm). A non-notched impact test was performed according to ISO179-1eA, with the sample dimensions of $80 \times 10 \times 4$ mm. The particle size distribution of WF was characterized on a Beckman-Coulter N4 Plus particle size analyzer (USA). After the steaming process and after the drying, the SWF was fully crumbed, with the aim of retaining the original shape of the SWF as much as possible. The WF and SWF were characterized in a dried state. Fourier transform infrared spectroscopy (FTIR) was carried out on a Nicolet 710 FTIR Spectrometer. For purifying purposes, the GPE were extracted using acetone in a Soxhlet extractor for 24 h and dried at 60°C until they had reached constant weight. Before testing, the specimens were compression-molded into tablets using KBr. In order to study the fracture surface morphology of the impacted specimens, the surface was sputtered with a thin layer of gold, and then scanning electron microscopy (SEM) was carried out on an S-550 SEM instrument made by Hitachi Co., Ltd., Japan. Differential Scanning Calorimetry (DSC) was carried out on a TA DSC 2910 by heating the sample to 200°C at calefactive rates of $10^\circ\text{C}/\text{min}$. The endothermic flows were recorded as a function of temperature. Thermogravimetric analysis (TGA) was carried out on a TA TGA 2050 instrument by heating the sample to 600°C at calefactive rates of $20^\circ\text{C}/\text{min}$. The weight loss percentage was recorded as a function of temperature. Vicat Softening Temperature (VST) analysis was carried out on RW-3 VST testing equipment made by Hebei Chengde Testing Machinery Inc., China. The water resistance was estimated by the water absorption (WA) as a function of time. Before testing the WA, the samples were dried at 60°C for 24 h, transferred to a dried ambience for cooling, and weighed to obtain their original weights (W_0). Then, the samples were immersed into water at ambient temperature. After a certain immersion time, the samples were weighed, and the immersed weights of the samples (W_t) were obtained. WA was determined by $WA = (W_t - W_0)/W_0 \times 100\%$. The WA testing lasted for 60 days. A dynamic rheological test was carried out on a RDA III Rheometmer (Rheometric Science Inc., USA). The dynamic rheological behavior was tested on a pair of circular plates with a diameter of 25 mm at 210°C . The gap between the two plates was set at 2.0 mm. The scanning frequency was 0.1 to 500 rad/s.

RESULTS AND DISCUSSION

Characterization of Wood Flours

Figure 1 and Table 1 demonstrate the effect of the steaming process on the particle sizes of WF. 93.5% of the WF particles were smaller than $100\ \mu\text{m}$, while only 62.2% of the SWF particles were smaller than $100\ \mu\text{m}$. 78.6% of the WF particles and 44.3% of the SWF particles were smaller than $50\ \mu\text{m}$. Note that all the WF particles were smaller than

400 μm , while there were some SWF particles larger than 400 μm but smaller than 1000 μm . The particle size characterization made it clear that the WF particles had been significantly enlarged by the steaming process.

Table 1. Particle Size Distribution and Weight Change in Wood Flour after Processing

Samples	Particle size distribution					Weight change		
	<1 μm	<10 μm	<20 μm	<50 μm	<100 μm	W ₁ (g)	W ₂ (g)	ΔW
WF	3.55%	25.9%	45.8%	78.6%	93.5%	48.5456	48.4785	0.0671
SWF	1.12%	9.55%	19.6%	44.3%	62.2%	109.7567	111.7000	1.9433

Note: For WF: W₁ and W₂ are the weights of wood flour before and after drying at 100 °C for 1 h, respectively. For SWF: W₁ and W₂ are the weights of wood flour before and after steaming at 100 °C for 1 h, respectively.

Because the particle size of the WF had been enlarged by the steaming process, the question to be further investigated was whether the steaming process caused any distinct change to the structure of the WF. The FTIR characterization helped to disclose these results, as shown in Fig. 2a. There were no obvious spectra differences between WF and SWF, except for the spectra in the range from 1800 cm^{-1} to 1000 cm^{-1} , which were attributed to primary compositions such as cellulose, hemicelluloses, and lignin (Ou *et al.* 2014b). In the Ou *et al.* (2014b) report, wood particles were treated to remove cellulose, hemicelluloses, and lignin, respectively. FTIR was used to characterize the variation in wood compositions. The wood particles extracted with individual composition showed peaks varying from 1800 cm^{-1} to 1000 cm^{-1} . In this research, the peaks for the SWF ranging from 1800 cm^{-1} to 1000 cm^{-1} , as shown in Fig. 2b, were wider than those of WF, as shown in Fig. 2a. Meanwhile, the peaks of SWF tended to shift to lower frequencies than those of WF. It is suggested that the primary compositions of WF were changed by the steaming process. The possible reason of the broadening and shifting of IR spectra is because of the increased hydrogen bonding in WF that was caused by water absorption and the changed structure of WF being opened to facilitate the interactions of polymers. However, the question to be further investigated was whether the steaming process really promoted the movement of primary components within the SWF. Figure 2b compares the DSC curves for WF and SWF. This curve was attributed to the glass transition enthalpy of the primary compositions in WF (Backman and Lindberg 2001). In the reports of Backman (Backman and Lindberg 2001) and Kelley (Kelley *et al.* 1987), both the DSC and dynamic mechanical thermal analysis (DMTA) results showed that wood has an α -peak from 30 °C to 60 °C, which represents the glass transition peak of primary compositions. These reports helped to identify the glass transition peak of the primary compositions that appeared at 36.2 °C in WF under natural state, as indicated in Fig. 2b. As depicted in Fig. 2b, the endothermic enthalpy of SWF (9.41 J/g) was higher than that of WF (7.25 J/g). The results made it clear that the chain segments of primary compositions in SWF were able to move more easily than those in WF. The steaming process is a popular method for drying wood (Ishikawa *et al.* 2004). Thus, the steaming process should be also an effective method for drying WF. This can be seen from Table 1. Table 1 compares the steaming process with the baking process in terms of their effects on the weight change of WF before and after these drying processes. The weight change for the WF following the baking process was only 0.0671 g,

while the weight change for the SWF following the steaming process was as high as 1.9433 g. The baking process hardly changed the weight of WF, while the steaming process noticeably changed the weight of SWF. The reason for this difference was that the baking process is unable to release the water trapped inside the WF cell walls, whereas the steaming process can release the water trapped inside the SWF cell walls (van Meel *et al.* 2011). The above results made it clear that the steaming process enlarged the voids in the SWF, activated the primary compositions in the SWF, and left the SWF drier than it left the WF, as is favorable for enhancing the interfacial interactions of rPE/SWF composites.

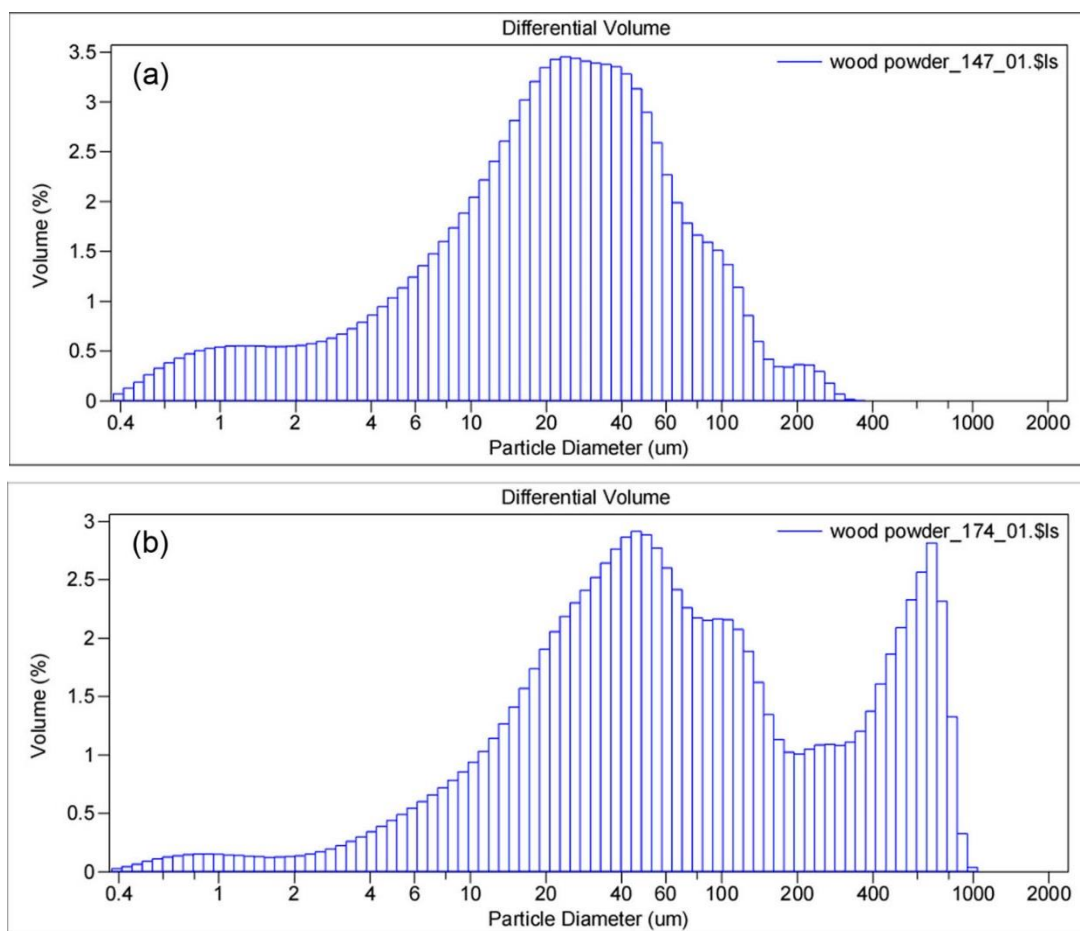


Fig. 1. The particle size change of wood flour (a) and steamed wood flour (b)

Morphology of rPE/WF Composites

Once the structural differences between WF and SWF had been clarified, a visualization of the correlative morphology of rPE/WF composites, manifesting as three lotus flowers at different florescence stages, was undertaken. Without compatibilizers, it was difficult for the polymer matrix to interact with the WF; thus, the rPE/WF composites were weakly compatible. The weakly compatible rPE/WF composites showed obvious interface fracture, and the voids could be seen on the WF surface. This weakly compatible interface of the composites resembled a fully blooming lotus, as shown in Fig. 3a. The WF particles corresponded to the seedpod of the lotus. The polymer matrix corresponded to the leaves of the lotus.

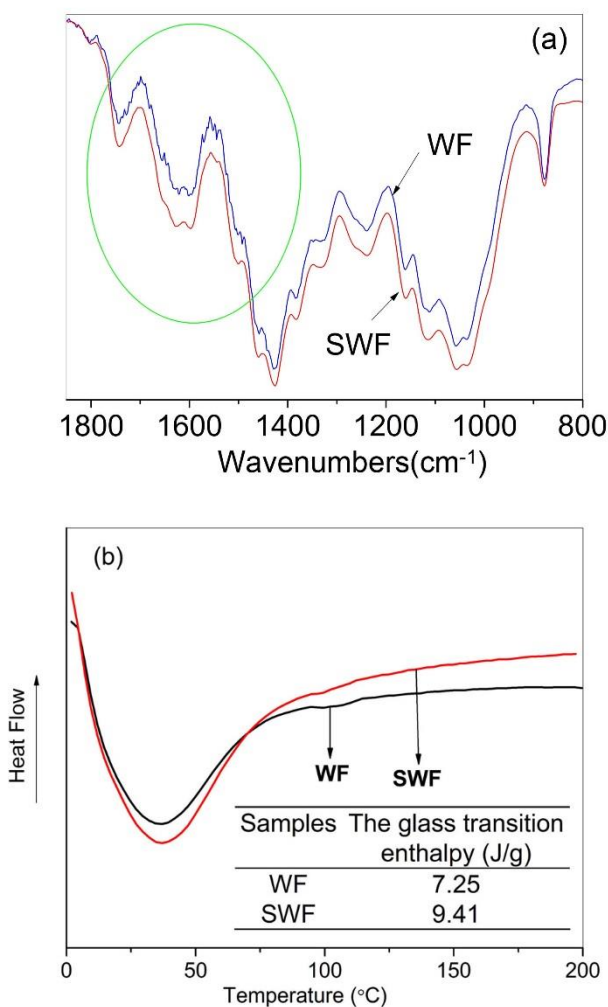


Fig. 2. The FTIR (a) and DSC (b) of wood flour

The seedpod-like WF particles broke away from the leaf-like polymer matrix. When GPE was used, GPE promoted the interaction of the polymer matrix with the WF. As shown in Fig. 3b, it was easier for the polymers to infiltrate into the voids and enwrap the surface of WF with the help of GPE. The interface of the composites did not show any distinct voids. It appeared that GPE had improved the interfacial interactions of the composites and therefore improved the interfacial compatibility. This compatible interface resembled a half-blooming lotus. The seedpod-like WF particles firmly interacted with the leaf-like polymer matrix.

When the WF was steamed, the voids of WF were enlarged. As shown in Fig. 3c, it was easier for the polymers to infiltrate into these voids and enwrap the SWF particles tightly. Therefore, the interfacial interactions were further enhanced. The interface of the composites resembled a budding lotus. The seedpod-like WF particle interacted with the leaf-like polymer matrix more firmly. These results revealed that rPE/SWF/GPE composites had better interfacial compatibility than did the other tested rPE/WF composites.

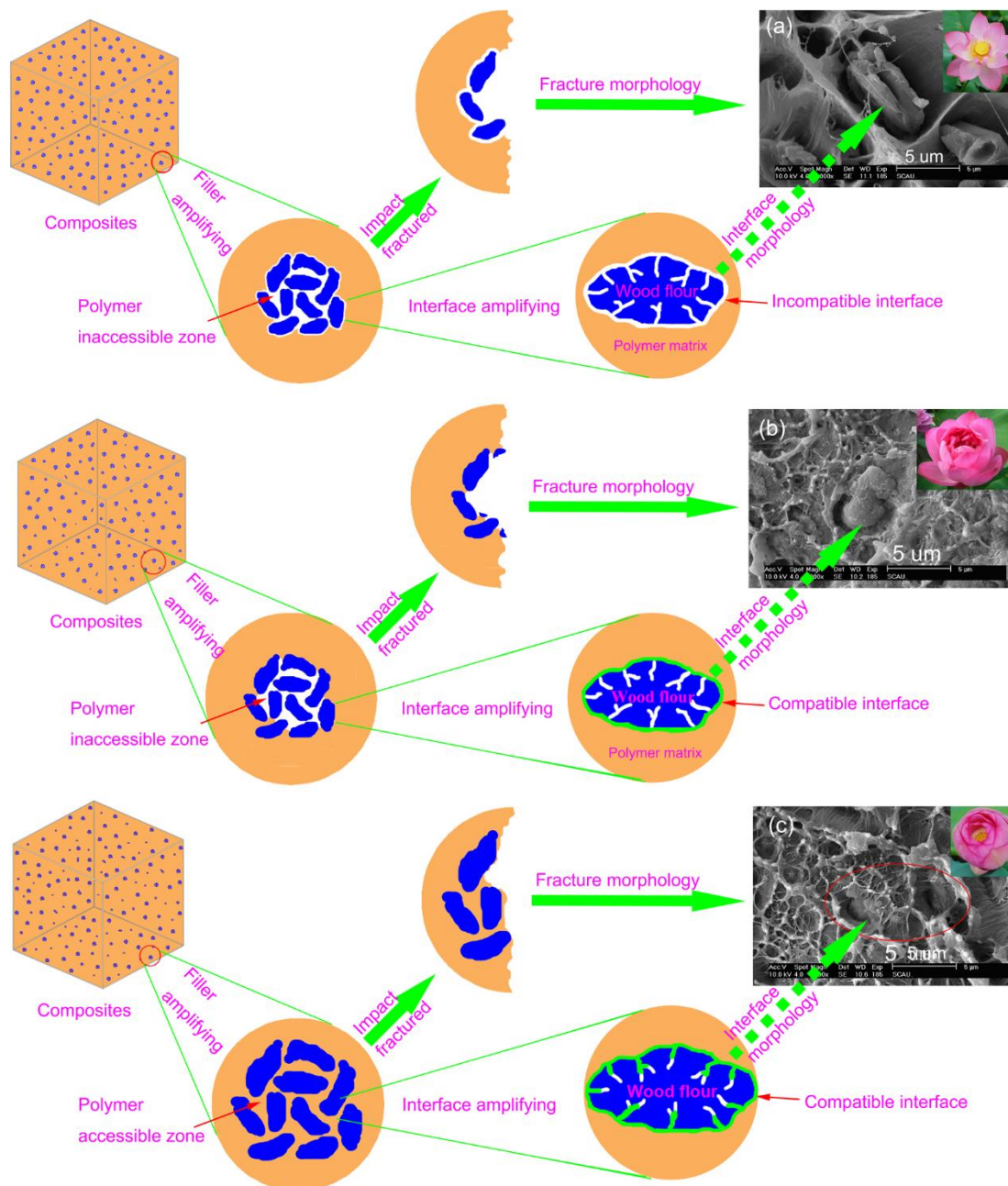


Fig. 3. The SEM morphology of rPE/WF composites: (a) rPE/WF (100/100), (b) rPE/WF/GPE (100/100/7), (c) rPE/SWF/GPE (100/100/7)

Interfacial Interaction Mechanism of rPE/WF Composites

Since the compatibility of the composites had been significantly improved, the nature of the interaction taking place between the graft copolymers and WF, which appeared to offer such fine compatibilization to the composites, was investigated. FTIR was used to characterize the structure of the purified GPE and GPW. It can be seen from Fig. 4 that three peaks appeared at 1781 cm^{-1} , 1732 cm^{-1} , and 1726 cm^{-1} , which were attributed to the stretching vibration of the grafted MAH, MMA, and BA, respectively. It could be inferred that the monomers had become grafted onto the powder PE or onto the melting PE wax. Since WF is a lignocellulosic fiber, it has many hydroxyl groups that

easily form chemical bonds with anhydride groups or isocyanate groups and form physical interactions with polar groups (Kazayawoko *et al.* 1999; Li and Matuana 2003; Lu *et al.* 2005). For this research, the suggested interfacial interaction mechanism of GPE to rPE/WF composites was that GPE afforded strong interfacial interactions between rPE and wood flour by chemically bonding with MAH or physically interacting with MMA and BA at the interfaces (Bledzki and Gassan 1999; Hong *et al.* 2014), as shown in Fig. 5. Since the voids of the WF had been enlarged by the steaming process, the steaming process facilitated the infiltration of the GPE into the voids of WF, which thereby supplemented the interfacial interactions. Through the enhanced compatibilization at these locations, the highly compatible rPE/wood flour composite was achieved.

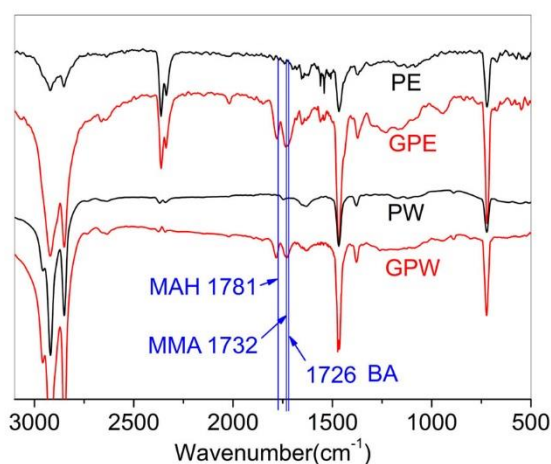


Fig. 4. FTIR of GPE and GPW

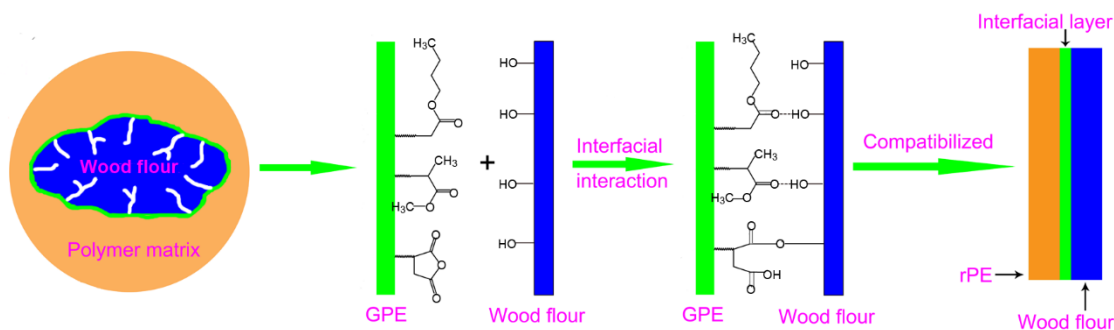


Fig. 5. The interfacial interaction mechanism of rPE/WF composites

Mechanical Properties of rPE/WF Composites

From the above characterization, it was clear that the GPE and the steaming process both improved the interfacial compatibility of the composites. However, the question to be further investigated was whether the improved interfacial compatibility could really result in the reinforcement of the composites. WF and SWF were used to prepare WPC. How they affected the performances of WPC was compared. As shown in Fig. 6, the loading of WF decrease the impact strength and tensile strength of the composites without any compatibilizers, though the flexural properties were maintained. When the GPE was loaded into the composites, the performances of the composites dramatically increased. The impact strength increased from 5.2 KJ/m² (rPE/WF) to 10.69 KJ/m² (rPE/WF/GPE). The

tensile strength increased from 20.16 MPa (rPE/WF) to 32.2 MPa (rPE/WF/GPE). The flexural strength increased from 30.56 MPa (rPE/WF) to 49.86 MPa (rPE/WF/GPE). The flexural modulus increased from 2054 MPa (rPE/WF) to 2501 MPa (rPE/WF/GPE). These results indicated that GPE had contributed to interfacial compatibilization and the resulted reinforcement of WPC. Note that the performance characteristics of rPE/SWF/GPE were higher than those of rPE/WF/GPE, except for the tensile strength, which did not change. The impact strength increased from 10.69 KJ/m² (rPE/WF/GPE) to 13.13 KJ/m² (rPE/SWF/GPE). The flexural strength increased from 49.86 MPa (rPE/WF) to 56.65 MPa (rPE/WF/GPE). The flexural strength increased from 2501 MPa (rPE/WF) to 3089 MPa (rPE/WF/GPE). It was obvious that the rPE/SWF/GPE system had the optimal performance among the compared composites. It is suggested that the steaming process promoted the sufficient infiltration of GPE into the inner voids of SWF and strongly enhanced the interfacial interactions of WPC. As a result, the mechanical properties of WPC were dramatically improved.

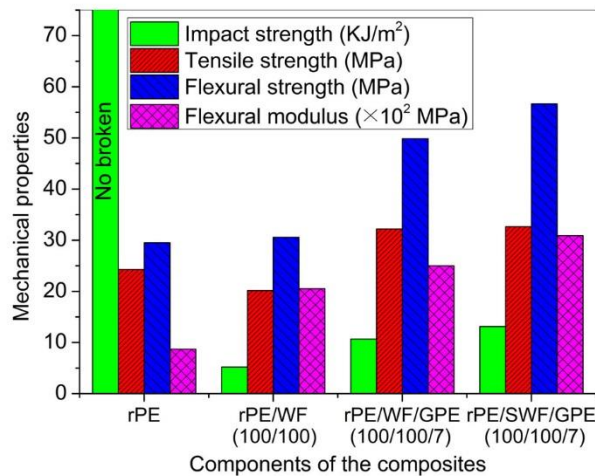


Fig. 6. The mechanical properties of rPE/WF composites

Water Resistance of rPE/WF Composites

Figure 7 depicts the water resistance of the rPE/WF composites.

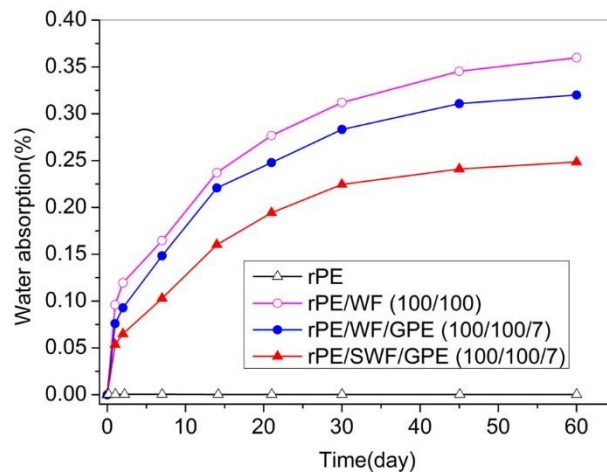


Fig. 7. The water resistance of rPE/WF composites

The rPE is a hydrophobic polymer. It has the lowest water absorption among the compared composites. The loading of WF dramatically increased the water absorption without any compatibilizers, while the loading of GPE significantly decreased the water absorption of the composites. Although the enlarged voids may have exposed the more hydrophilic groups, these voids were more easily enwrapped by the polymer matrix and GPE, which protected them from water attack. Therefore, the water resistance of rPE/SWF/GPE composites was better than that of rPE/WF/GPE composites.

Thermal Stability of rPE/WF Composites

Figures 8 and 9 depict the thermal stability of the rPE/WF composites in terms of TGA and Vicat softening temperature, respectively. Since the major compositions of the composites were similar, samples 2, 3, and 4 show similar shapes, as shown in Fig. 8.

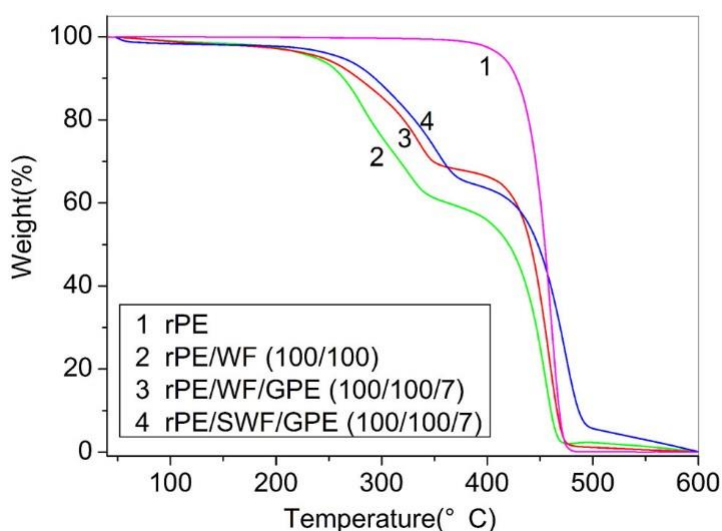


Fig. 8. The TGA curves of rPE/WF composites

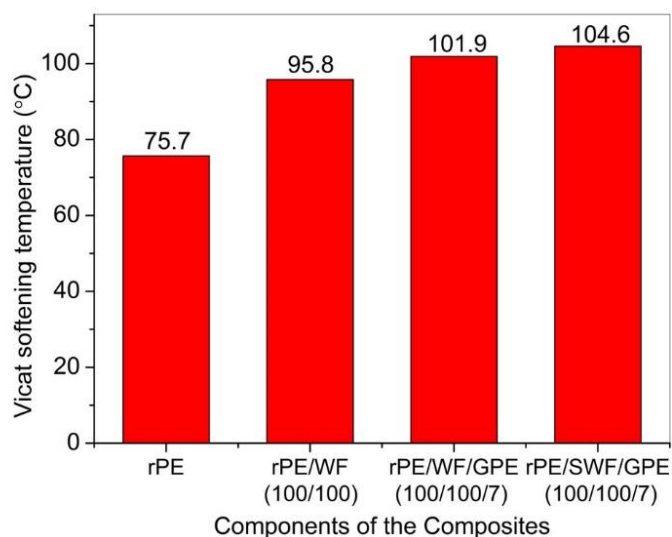


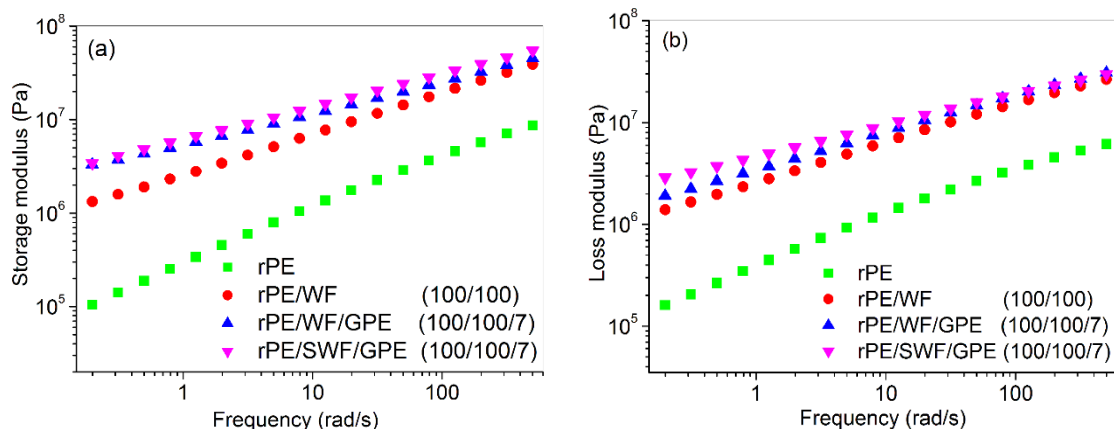
Fig. 9. The Vicat softening temperature of rPE/WF composites

The rPE/WF composites showed a tiny weight loss near 100 °C and two primary weight loss regions in the ranges of 220 to 350 °C and 350 to 480 °C, respectively. The tiny weight loss was attributed to the moisture and volatile substances. The weight loss in the first range was attributed to primarily hemicelluloses, lignin, and cellulose (Shebani *et al.* 2008). The weight loss in the second range was attributed primarily to the degradation of rPE.

The thermal stability of the rPE/WF/GPE composites was higher than that of the rPE/WF composites. The thermal stability of the rPE/SWF/GPE composites was significantly higher than that of the rPE/WF/GPE composites. This was attributed to the enhanced interfacial interactions brought about by the steaming process. Similar results were found for the VST, as shown in Fig. 9. The VST of the rPE/WF composites (95.8 °C) was much higher than that of the rPE (75.7 °C), indicating that the WF contributed to the thermal stability of the rPE/WF composites. The VST of the rPE/WF/GPE composites (101.9 °C) was higher than that of the rPE/WF, suggesting that the GPE contributed significantly to the thermal stability of the rPE/WF composites. The VST of the rPE/SWF/GPE composites (104.6 °C) was higher than that of the rPE/WF/GPE composites, suggesting that the steaming process also significantly enhanced the thermal stability of the compatibilized composites.

Rheological Analysis of rPE/WF Composites

Figure 10 depicts the dynamic rheological properties of rPE/WF composites. The loadings of WF and GPE both increased the storage modulus and loss modulus of the composites, respectively. It appeared that WF and GPE both contributed to the reinforcement of the composites.



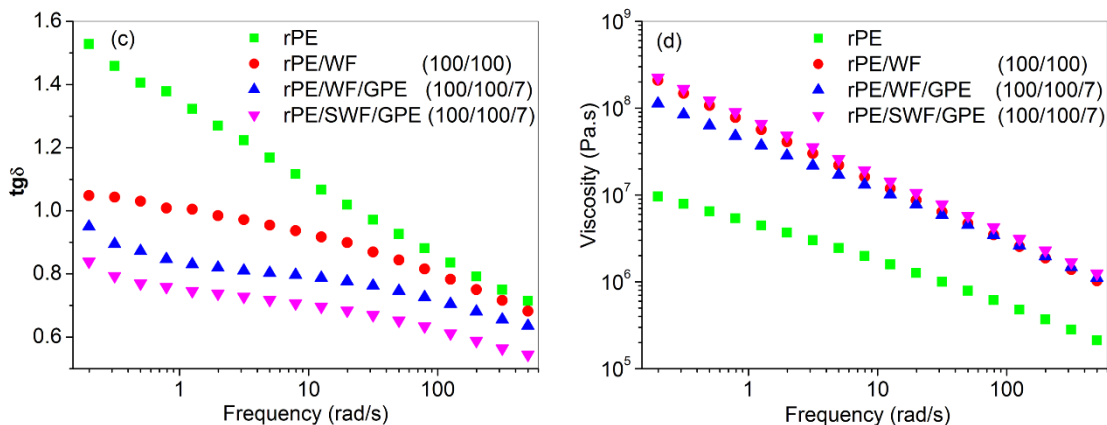


Fig. 10. The dynamic rheological properties of rPE/WF composites

As for the viscosity, while the loading of WF increased the viscosity of the composites, the presence of GPE did not dramatically change the viscosity of the composites. Though the viscosity was hardly affected by the GPE, the loss factors ($\tan \delta$, given as the ratio of loss modulus to storage modulus) of the rPE/WF/GPE composites were lower than those of rPE/WF composites. The reason for this was that GPE has a high graft degree and long grafted side chains. The high graft degree enhanced the interfacial interactions and resulted in an increase in viscosity. The long grafted side chains played the role of plasticizer, resulting in a decrease in the viscosity (Jia *et al.* 2000; Hong *et al.* 2014). The neutralizing effect of the high graft degree and long grafted side chains kept the viscosity invariant. Since the steaming process enhanced the interfacial interactions, it also increased the storage modulus and loss modulus of the composites. Note that the steaming process did not dramatically increase the viscosity of the composites, but significantly decreased the $\tan \delta$ of the composites. This occurred because the steaming process not only extended the interfacial interactions into the voids of SWF, but also extended the plasticization of the GPE into the composites, consequently decreasing the $\tan \delta$ of the rPE/SWF/GPE composites. This indicated that a combination of the GPE and the steaming process was favorable to the dynamic rheological properties of the composites.

CONCLUSIONS

1. The steaming process enlarged the voids in SWF, activated the primary compositions in SWF, and made SWF dryer than WF, which was favorable for enhancing the interfacial interactions and therefore improving the performances of rPE/SWF composites.
2. The interfacial morphology of the composites depended upon the interfacial compatibility of the composites. Without GPE, a compatibilizer, the interface of the weakly compatible composites resembled a full blooming lotus. When compatibilized by GPE, the interface of the compatible composites resembled a half blooming lotus. Following steam treatment, the interface of the enhanced compatible composites resembled a budding lotus.
3. With the help of GPE, the steaming process was able to further enhance the interfacial compatibility of the composites and improve the mechanical properties, water

resistance, and thermal stability of the composites. In addition, the steaming process showed itself to be favorable to the dynamic rheological properties of the composites.

4. GPE was able to notably improve the interfacial compatibility of the composites, and therefore improve the mechanical properties, water resistance, thermal stability, and dynamic rheological properties of the composites.

ACKNOWLEDGMENTS

This work was funded by the National Natural Science Foundation of China (Grant No. 51276044), the Research Fund of Young Teachers for the Doctoral Program of Higher Education of China (Grant No. 20134420120009), the Special Program for Public Interest Research and Capability Construction of Guangdong Province (Grant No. 2014A010105047), the Science and Technology Program of Guangdong Province (Grant No. 2013B051000077), the Science and Technology Program of Guangzhou City (Grant No. 201508030018), and the PhD Scientific Research Startup Fund of GDUT (Grant No. 12ZK0063).

REFERENCES CITED

- Artzi, N., Nir, Y., Narkis, M., and Siegma, A. (2003). "The effect of maleated compatibilizers on the structure and properties of EVOH/clay nanocomposites," *Polymer Composites* 24(5), 627-639. DOI: 10.1002/pc.10058
- Ashori, A., and Nourbakhsh, A. (2009). "Characteristics of wood-fiber plastic composites made of recycled materials," *Waste Management* 29(4), 1291-1295. DOI: 10.1016/j.wasman.2008.09.012
- Ashori, A. (2008). "Wood-plastic composites as promising green composites for automotive industries," *Bioresource Technology* 99(11), 4661-4667. DOI: 10.1016/j.biortech.2007.09.043
- Aziz, S. H., and Ansell, M. P. (2004). "The effect of alkalization and fibre alignment on the mechanical and thermal properties of kenaf and hemp bast fibre composites: Part 1: Polyester resin matrix," *Composites Science and Technology* 64(9), 1219-1230. DOI: 10.1016/j.compscitech.2003.10.001
- Backman, A. C., and Lindberg, K. A. H. (2001). "Difference in wood material responses for radial and tangential direction as measured by dynamic mechanical thermal analysis," *Journal of Materials Science* 36(15), 3777-3783. DOI: 10.1023/A:1017986119559
- Bengtsson, M., Baillif, M. L., and Oksman, K. (2007). "Extrusion and mechanical properties of highly filled cellulose fibre-polypropylene composites," *Composites Part A: Applied Science and Manufacturing* 38(8), 1922-1931. DOI: 10.1016/j.compositesa.2007.03.004
- Bledzki, A. K., and Gassan, J. (1999). "Composites reinforced with cellulose based fibres," *Progress in Polymer Science* 24(2), 221-274. DOI: 10.1016/S0079-6700(98)00018-5
- Danyadi, L., Janecska, T., Szabo, Z., Nagy, G., Moczó, J., and Pukanszky, B. (2007). "Wood flour-filled PP composites: Compatibilization and adhesion," *Composite Science and Technology* 67, 2838-2846. DOI: 10.1016/j.compscitech.2007.01.024

- Demir, H., Atikler, U., Balkose, D., and Tihminlioglu, F. (2006). "The effect of fiber surface treatments on the tensile and water sorption properties of polypropylene-luffa fiber composites," *Composites Part A: Applied Science and Manufacturing* 37(3), 447-456. DOI: 10.1016/j.compositesa.2005.05.036
- Ding, C., Jia, D. M., He, H., Guo, B. C., and Hong, H. Q. (2005). "How organo-montmorillonite truly affects the structure and properties of polypropylene," *Polymer Testing* 24(1), 94-100. DOI: 10.1016/j.polymertesting.2004.06.005
- Fang, Y. Q., Wang, Q. W., Guo, C. G., Song, Y. M., and Cooper, P. A. (2013). "Effect of zinc borate and wood flour on thermal degradation and fire retardancy of polyvinyl chloride (PVC) composites," *Journal of Analytical and Applied Pyrolysis* 100, 230-236. DOI: 10.1016/j.jaap.2012.12.028
- Gao, H., Xie, Y. J., Ou, R. X., and Wang, Q. W. (2012). "Grafting effects of polypropylene/polyethylene blends with maleic anhydride on the properties of the resulting wood-plastic composites," *Composites Part A: Applied Science and Manufacturing* 43(1), 150-157. DOI: 10.1016/j.compositesa.2011.10.001
- Guo, C. G., Ma, L. C., Sun, C. Y., and Li, L. P. (2013). "Influence of high loaded wood flour and coupling agent (m-TMI-g-PP) content on properties of wood flour/polypropylene," *Journal of Adhesion Science and Technology* 27(3), 912-923. DOI: 10.1080/01694243.2012.727163
- Guo, C. G., and Wang, Q. W. (2008). "Influence of m-isopropenyl- α,α -dimethylbenzyl isocyanate grafted polypropylene on the interfacial interaction of wood-flour/polypropylene composites," *Journal of Applied Polymer Science* 109(5), 3080-3086. DOI: 10.1002/app.27800
- Hoang, T., Chinh, N. T., Trang, N. T. T., Hang, T. T. X., Thanh, D. T. M., Hung, D. V., Ha, C. S., and Aufray, M. (2013). "Effects of maleic anhydride grafted ethylene/vinyl acetate copolymer (EVA) on the properties of EVA/silica nanocomposites," *Macromolular Research* 21(11), 1210-1217. DOI: 10.1007/s13233-013-1157-8
- Hong, H. Q., Liao, H. Y., Zhang, H. Y., He, H., Liu, T., and Jia, D. M. (2014). "Significant improvement in performance of recycled polyethylene/wood flour composites by synergistic compatibilization at multi-scale interfaces," *Composites Part A: Applied Science and Manufacturing* 64, 90-98. DOI: 10.1016/j.compositesa.2014.04.022
- Hong, H. Q., Liu, T., He, H., Jia, D. M., and Zhang, H. Y. (2011). "Effect of interfacial modifiers on physical properties and flammability properties of PE/wood composites," *Polymers & Polymer Composites* 19(8), 639-645.
- Hong, H. Q., Xu, H. X., He, H., Liu, T., and Jia, D. M. (2009). "Effect of ternary monomer graft copolymers on morphology and properties of rice chaff filled polypropylene composites," *Plastics, Rubber, and Composites* 38(1), 21-26. DOI: 10.1179/174328909X387720
- Ishikawa, A., Kuroda, N., and Kato, A. (2004). "In situ measurement of wood moisture content in high-temperature steam," *Journal of Wood Science* 50, 7-14. DOI: 10.1007/s10086-003-0521-2
- Jia, D. M., Luo, Y. F., Li, Y. M., Lv, H., Fu, W. W., and Cheung, W. L. (2000). "Synthesis and characterization of solid-phase graft copolymer of polypropylene with styrene and maleic anhydride," *Journal of Applied Polymer Science* 78(14), 2482-2487. DOI: 10.1002/1097-4628(20001227)78:14<2482::AID-APP70>3.0.CO;2-#

- Kazayawoko, M., Balatinecz, J. J., and Matuana, L. M. (1999). "Surface modification and adhesion mechanisms in wood fiber-polypropylene composites," *Journal of Materials Science* 34(24), 6189-6199. DOI: 10.1023/A:1004790409158
- Kelley, S. S., Rials, T. G., and Glasser, W. G. (1987). "Relaxation behaviour of the amorphous components of wood," *Journal of Materials Science* 22(2), 617-624. DOI: 10.1007/BF01160778
- Lashgari, S., Garmabi, H., Lashgari, S., and Mohammadian-Gezaz, S. (2011). "Improving the interfacial adhesion of highly filled PP-bagasse composites designed by taguchi method," *Journal of Thermoplastic Composite Materials* 24(4), 431-446. DOI: 10.1177/0892705710387982
- Li, Q., and Matuana, L. M. (2003). "Effectiveness of maleated and acrylic acid-functionalized polyolefin coupling agents for HDPE-wood-flour composites," *Journal of Thermoplastic Composite Materials* 16(6), 551-564. DOI: 10.1177/089270503033340
- Li, X., Tabil, L. G., and Panigrahi, S. (2007). "Chemical treatments of natural fiber for use in natural fiber-reinforced composites: A review," *Journal of Polymers and the Environment* 15(1), 25-33. DOI: 10.1007/s10924-006-0042-3
- Li, Y., Xie, X. M., and Guo, B. H. (2001). "Study on styrene-assisted melt free-radical grafting of maleic anhydride onto polypropylene," *Polymer* 42(8), 3419-3425. DOI: 10.1016/S0032-3861(00)00767-9
- Li, Z. W., Gao, H., and Wang, Q. W. (2012). "Preparation of highly filled wood flour/recycled high density polyethylene composites by *in situ* reactive extrusion," *Journal of Applied Polymer Science* 124(6), 5247-5253. DOI: 10.1002/app.34233
- Liu, R., Peng, Y., Cao, J., and Chen, Y. (2014). "Comparison on properties of lignocellulosic flour/polymer composites by using wood, cellulose, and lignin flours as fillers," *Composites Science and Technology* 103(28), 1-7. DOI: 10.1016/j.compscitech.2014.08.005
- Lu, J. Z., Negulescu, I. I., and Wu, Q. L. (2005). "Maleated wood-fiber/high-density-polyethylene composites: Coupling mechanisms and interfacial characterization," *Composite Interfaces* 12(1-2), 125-140. DOI: 10.1163/1568554053542133
- Luo, S. P., Cao, J. Z., and Peng, Y. (2014). "Properties of glycerin-thermally modified wood flour/polypropylene composite," *Polymer Composites* 35(2), 201-207. DOI: 10.1002/pc.22651
- Manchado, M. A. L., Arroyo, M., Biagiotti, J., and Kenny, J. M. (2003). "Enhancement of mechanical properties and interfacial adhesion of PP/EPDM/flax fiber composites using maleic anhydride as a compatibilizer," *Journal of Applied Polymer Science* 90(8), 2170-2178. DOI: 10.1002/app.12866
- Mansour, S. H., El-Nashar, D. E., and Abd-El-Messieh, S. L. (2006). "Effect of chemical treatment of wood flour on the properties of styrene butadiene rubber/polystyrene composites," *Journal of Applied Polymer Science* 102(6), 5861-5870. DOI: 10.1002/app.24984
- Mbarek, T. B., Robert, L., Sammouda, H., Charrier, B., Orteu, J. J., and Hugot, F. (2013). "Effect of acetylation and additive on the tensile properties of wood fiber-high-density polyethylene composite," *Journal of Reinforced Plastics and Composites* 32(21), 1646-1655. DOI: 10.1177/0731684413505256
- Nair, K. C., and Thomas, S. (2003). "Effect of interface modification on the mechanical properties of polystyrene-sisal fiber composites," *Polymer Composites* 24(3), 332-343. DOI: 10.1002/pc.10033

- Najafi, S. K. (2013). "Use of recycled plastics in wood plastic composites – A review," *Waste Management* 33(9), 1898-1905. DOI: 10.1016/j.wasman.2013.05.017
- Ou, R. X., Xie, Y. J., Wolcott, M. P., Sui, S. J., and Wang, Q. W. (2014a). "Morphology, mechanical properties, and dimensional stability of wood particle/high density polyethylene composites: Effect of removal of wood cell wall composition," *Materials & Design* 58, 339-345. DOI: 10.1016/j.matdes.2014.02.018
- Ou, R. X., Xie, Y. J., Wolcott, M. P., Yuan, F. P., and Wang, Q. W. (2014b). "Effect of wood cell wall composition on the rheological properties of wood particle/high density polyethylene composites," *Composites Science and Technology* 93, 68-75. DOI: 10.1016/j.compscitech.2014.01.001
- Ou, R. X., Zhao, H., Sui, S. J., Song, Y. M., and Wang, Q. W. (2010). "Reinforcing effects of Kevlar fiber on the mechanical properties of wood-flour/high-density-polyethylene composites," *Composites Part A: Applied Science and Manufacturing* 41(9), 1272-1278. DOI: 10.1016/j.compositesa.2010.05.011
- Shebani, A. N., van Reenen, A. J., and Meincken, M. (2008). "The effect of wood extractives on the thermal stability of different wood species," *Thermochimica Acta* 471(1-2), 43-50. DOI: 10.1016/j.tca.2008.02.020
- Thompson, R. C., Moore, C. J., Vom, S. F. S., and Swan, S. H. (2009). "Plastics, the environment and human health: Current consensus and future trends," *Philosophical Transactions of the Royal Society B: Biological Sciences* 364(1526), 2153-2166. DOI: 10.1098/rstb.2009.0053
- van Meel, P. A., Erich, S. J. F., Huinink, H. P., Kopinga, K., de Jong, J., and Adan, O. C. G. (2011). "Moisture transport in coated wood," *Progress in Organic Coatings* 72(4), 686-694. DOI: 10.1016/j.porgcoat.2011.07.011
- Wu, Q. L., Chi, K., Wu, Y. Q., and Lee, S. (2014). "Mechanical, thermal expansion, and flammability properties of co-extruded wood polymer composites with basalt fiber reinforced shells," *Materials & Design* 60, 334-342. DOI: 10.1016/j.matdes.2014.04.010
- Xu, Y. J., Wu, Q. L., Lei, Y., and Yao, F. (2010). "Creep behavior of bagasse fiber reinforced polymer composites," *Bioresource Technology* 101(9), 3280-3286. DOI: 10.1016/j.biortech.2009.12.072
- Yeh, S. K., Kim, K. J., and Gupta, R. K. (2013). "Synergistic effect of coupling agents on polypropylene-based wood-plastic composites," *Journal of Applied Polymer Science* 127(2), 1047-1053. DOI: 10.1002/app.37775
- Zafeiropoulos, N. E., Williams, D. R., Baillie, C. A., and Matthews, F. L. (2002). "Engineering and characterisation of the interface in flax fibre/polypropylene composite materials. Part I. Development and investigation of surface treatments," *Composites Part A: Applied Science and Manufacturing* 33(3), 1083-1093. DOI: 10.1016/S1359-835X(02)00082-9
- Zhou, Z. F., Xu, M., Yang, Z. Z., Li, X. X., and Shao, D. W. (2014). "Effect of maleic anhydride grafted polyethylene on the properties of chopped carbon fiber/wood plastic composites," *Journal of Reinforced Plastics and Composites* 33(13), 1216-1225. DOI: 10.1177/0731684414531633

Article submitted: June 25, 2015; Peer review completed: September 7, 2015; Revised version received: September 11, 2015; Accepted: September 12, 2015; Published: October 5, 2015.

DOI: 10.15376/biores.10.4.7817-7833